ESC-TR-98-045

Technical Report
1052

Background Fluorescence in an Aerosol Biodetector Based on 266-nm Excitation

R.L. Aggarwal

17 May 1999

Lincoln Laboratory
MASSACHUSETTS INSTITUTE OF TECHNOLOGY
LEXINGTON, MASSACHUSETTS

Prepared for the Department of the Army
under Air Force Contract F19628-95-C-0002.

This report is based on studies performed at Lincoln Laboratory, a center for research operated by Massachusetts Institute of Technology. This work was sponsored by the Department of the Army, ERDEC, under Air Force Contract F19628-95-C-0002.

The ESC Public Affairs Office has reviewed this report, and it is releasable to the National Technical Information Service, where it will be available to the general public, including foreign nationals.

This technical report has been reviewed and is approved for publication.

FOR THE COMMANDER

Gary Tatungian
Administrative Contracting Officer
Contracted Support Management

Non-Lincoln Recipients

PLEASE DO NOT RETURN

Permission is given to destroy this document when it is no longer needed.

MASSACHUSETTS INSTITUTE OF TECHNOLOGY
LINCOLN LABORATORY

BACKGROUND FLUORESCENCE IN AN AEROSOL BIODETECTOR BASED ON 266-nm EXCITATION

R.L. AGGARWAL
Group 82

TECHNICAL REPORT 1052

17 MAY 1999

LEXINGTON MASSACHUSETTS

ABSTRACT

Background fluorescence in an aerosol biodetector based on 266-nm excitation has been investigated, using a gas cell which could be evacuated and then filled with a gas (of interest) at a known pressure. A frequency-quadrupled, Q-switched Nd:YAG microchip laser with a pulse width of less than 1 ns and a pulse repetition rate of ~10^4 pps was used to measure both fluorescence and Rayleigh scattering in a direction at 90° to the 266-nm excitation beam, as a function of the gas pressure for nitrogen, oxygen, and room air. Rayleigh scattering was also measured for helium and xenon gases. The relative Rayleigh scattering cross sections measured in this work are consistent with their previously reported values, ensuring that the observed fluorescence was originating from a region of the gas in the direct path of the 266-nm excitation beam. Fluorescence signal observed in the spectral range of interest 300–650 nm under nominal vacuum conditions (~1×10^{-5} torr) exhibited strong quenching upon filling the gas cell with oxygen, but not with nitrogen. Strong oxygen-induced quenching leads us to believe that the background fluorescence is due, at least in part, to the presence of residual hydrocarbons in the atmospheric air. An order-of-magnitude calculation, based on an estimated value of fluorescence cross section of 1×10^{-21} cm^2, oxygen quenching factor of 0.2 for atmospheric air, and concentration of 10 ppb for hydrocarbons in urban air, is consistent with the observed value of ~4 photons per excitation pulse for the background fluorescence signal in our single-pass biodetector with f# of ~1 and 266-nm pulse energy of ~200 nJ.

ACKNOWLEDGMENTS

The author would like to thank Prof. L. A. Melton, Drs. T. H. Jeys, A. Sanchez, and T. Y. Fan for technical discussions, S. DiCecca for providing results of his previous work on the subject, P. W. O'Brien for assistance with data on Rayleigh scattering, and R. Thomson for providing the EPA data.

TABLE OF CONTENTS

LIST OF ILLUSTRATIONS

LIST OF TABLES

1. INTRODUCTION

Background fluorescence has been recognized as a major source of noise in our aerosol biodetector based on 266-nm excitation radiation, provided by a frequency-quadrupled, Q-switched Nd:YAG microchip laser with a pulse width of less than 1 ns, and pulse repetition rate of approximately 10^4 pulses per second. The spectral range of interest for fluorescence in our biodetector extends from approximately 300 nm to 650 nm. In order to determine the source of the background fluorescence, we have measured Rayleigh scattering and fluorescence from nitrogen, oxygen, or room air excited with 266-nm Q-switched pulses, using a gas cell which could be evacuated and then filled with the appropriate gas. The results of this study suggest that the background fluorescence in our aerosol biodetector may, in part, be due to the presence of hydrocarbons in the air.

2. EXPERIMENTAL

The experimental setup for the Rayleigh scattering and fluorescence measurements is shown in Figure 1. It consists of a 2-in diameter stainless steel gas cell, equipped with a UV grade fused silica (Supersil 1) Brewster window on one end and a normal-incidence UV grade fused silica window on the other end for the 266-nm excitation beam to pass through the gas cell. Another normal-incidence UV grade fused silica window is mounted on the gas cell for the transmission of the fluorescence and/or Rayleigh scattering in a direction at 90° to the 266-nm excitation beam. The gas cell is also connected to a vacuum pump, gas inlet manifold, and pressure gauge. The 90° Rayleigh scatterting and/or fluorescence is focused by a 1-in diameter, 1-in focal length fused silica biconvex lens on a slit placed in front of an 8-mm diameter photomultiplier tube, Hamamatsu model H5783-03, with spectral response from 185 to 650 nm. The length and width of the slit are 10 mm and 1 mm, parallel and perpendicular to the plane of the figure, respectively. The focusing lens is at a distance of ~3 in from the 266-nm excitation beam and ~1.5 in from the slit; this implies that the image of the excitation beam at the slit is reduced in size by a factor of 2 in each dimension. The clear aperture of the lens is 7/8 in so that the effective f-number of the lens is 3.4. For fluorescence measurements, two Schott glass long-wave pass filters, WG 295 (50% transmission point at 295 nm), are placed in front of the slit for blocking the scattered 266-nm radiation. A 350-MHz digital oscilloscope, LeCroy model 9450, is connected to the output of the photomultiplier tube for Rayleigh scattering measurements, and to a Stanford Research Systems gated photon counter model SR400 for luminescence measurements.

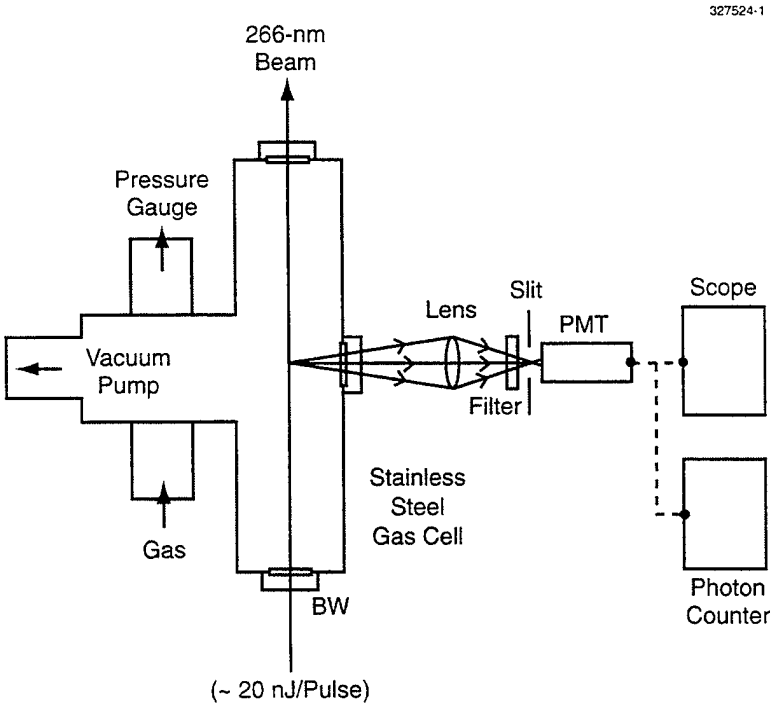

Figure 1. Schematic of the experimental setup showing the gas cell, 266-nm excitation beam, lens for focusing fluorescence and/or Rayleigh-scattered radiation onto a slit placed in front of a photomultiplier tube, long-wave pass filters, digital oscilloscope, and a photon counter.

The trigger signal for the oscilloscope and the photon counter is provided by a silcon photodiode exposed to a small fraction of light from a beam splitter placed in the path of the 266-nm excitation beam. The excitation beam is largely s-polarized, i.e., the electric vector of the excitation radiation is perpendicular to the plane of Rayleigh scattering which is also the plane of Figure 1. The diameter of the excitation beam was estimated to be ~2 mm, and the energy of the input beam was measured to be ~20 nJ per pulse.

3. RAYLEIGH SCATTERING

Theory for the scattering of light by small particles was first given by Lord Rayleigh [1] in 1871. Rayleigh scattering [1–3] is an elastic scattering process, i.e., the scattered radiation has the same wavelength as that of the excitation radiation. Rayleigh scattering cross section is inversersely proportional to the fourth power of the wavelength of the excitation radiation, and the scattering cross section is isotropic for s-polarization excitation. Measured values for Rayleigh scattering cross sections in the visible and ultraviolet regions have been reported by Rudder and Bach [4], and by Shardanand and Rao [5], for a number of gas molecules including O_2 and N_2. It is precisely for this reason that we chose to measure Rayleigh scattering in this work. At 266 nm, the Rayleigh scattering cross section for N_2 at normal temperature and pressure (NTP) is 0.96×10^{-25} cm^2, as reported by Bates [6].

Figure 2 shows a trace of the Rayleigh scattering signal from atmospheric air in the gas cell, as recorded by the LeCroy oscilloscope, using 800 V for the supply voltage for the photomultiplier tube and 50 ohm load impedence. The full width at half-maximum (FWHM) of the observed signal is ~2.5 ns, consistent with that expected from the bandwidth of the measuring system including the photomultiplier tube, the oscilloscope, and the pulse width of the excitation beam.

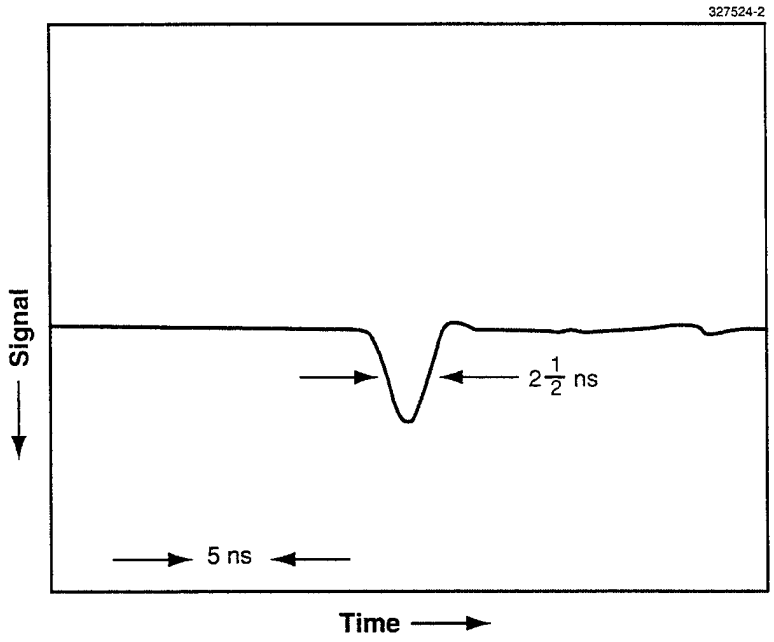

Figure 2. A trace of the Rayleigh scattering signal from atmospheric air in the gas cell at room temperature, showing the full width at half-maximum (FWHM) of ~2.5 ns.

The value of the peak signal in Figure 2 is 29 mV which corresponds to a peak anode current for the photomultiplier tube of 6×10^{-4} A. The typical anode current responsivity of the photomultiplier tube at 266 nm is 6×10^{3} A/W for a supply voltage of 800 V. This implies that the Rayleigh scattering pulse incident on the photomultiplier tube has a peak power of 1×10^{-7} W. Using the observed value of 2.5 ns for FWHM, we deduce a value of 2.5×10^{-7} nJ for the Rayleigh scattering pulse energy incident upon the photomultiplier tube. Thus the observed Rayleigh scattering efficiency η_R for our system is equal to 1.3×10^{-8}, using a value of 20 nJ for the energy of the 266-nm excitation pulse. An expected value for the Rayleigh scattering efficiency may be calculated from the following realtionship:

$$\eta_R = (\sigma_R L n_g) T_W T_L F_{sp} / [16(f\#)^2] \ , \qquad (1)$$

where σ_R is the Raman scattering cross section, L is the effective length of the excitation beam imaged on the slit, n_g is the molecular concentration of the gas, T_W is the transmission of the side window on the gas cell, T_L is the transmission of the focusing lens, F_{sp} is the fraction of the excitation pulse energy with s-polarization, and f# is the f-number of the lens. Using the values $\sigma_R = 0.96 \times 10^{-25}$ cm^2 for air, L = 1.6 cm, $n_g = 2.5 \times 10^{19}$ cm^{-3}, $T_W = T_L = 0.92$, $F_{sp} = 0.8$, and f# = 3.4, we calculate a value of 1.4×10^{-8} for η_R, in good agreement with the measured value of 1.3×10^{-8}. However, such a good agreement may be fortuitous because the current responsivity for the photomultiplier tube can be more than a factor of 2 different than its typical value (provided by the manufacturer) used in this calculation.

Rayleigh scattering cross sections were measured for O_2, He, and Xe relative to that for N_2. The relative scattering cross sections measured in this work are consistent with their known values, as given below in Table 1.

TABLE 1

Relative Rayleigh Scattering Cross Sections for N_2, O_2, He, and Xe

Gas	This work	Previous
N_2	1	1
O_2	0.84	0.85 [5]
He	0.01	0.014 [4,5]
Xe	5.4	5.42 [4]

4. FLUORESCENCE

Rationale for measuring Rayleigh scattering in this work was to make sure that the light originating from the region of the excitation beam was focused on the slit placed in front of the photomultiplier tube. This is important because fluorescence can also arise from the walls of the gas cell due to scattered light incident upon the walls.

Fluorescence signals observed in this work were orders of magnitude weaker compared to Rayleigh scattering signals. The probability for the detection of a single fluorescence photon by the photomultiplier tube was of the order of 10^{-3} per 266-nm excitation pulse with ~3×10^{10} photons. Therefore, we used a gated photon counter to count the current pulses from the photomultiplier assumed to arise from a single fluorescence photon in a given excitation pulse.

Figure 3 shows variation of the observed fluorescence signal in terms of photomultiplier counts/1000 excitation pulses with pressure from nominal vacuum to 750 torr of oxygen, nitrogen, and room air. The data shown in Figure 3 were obtained with a supply voltage of 900 V for the photomultiplier, a discrimination level of 2.5 mV, and a gate width of 40 ns for the gated photon counter; the start of the gate was adjusted so as to maximize the fluorescence signal. The observed fluorescence shows a significant decrease with increase in pressure of room air as well as with pressure of oxygen. On the other hand, the observed fluorescence shows a small increase with pressure of nitrogen. These results indicate that the observed fluorescence is quenched by oxygen.

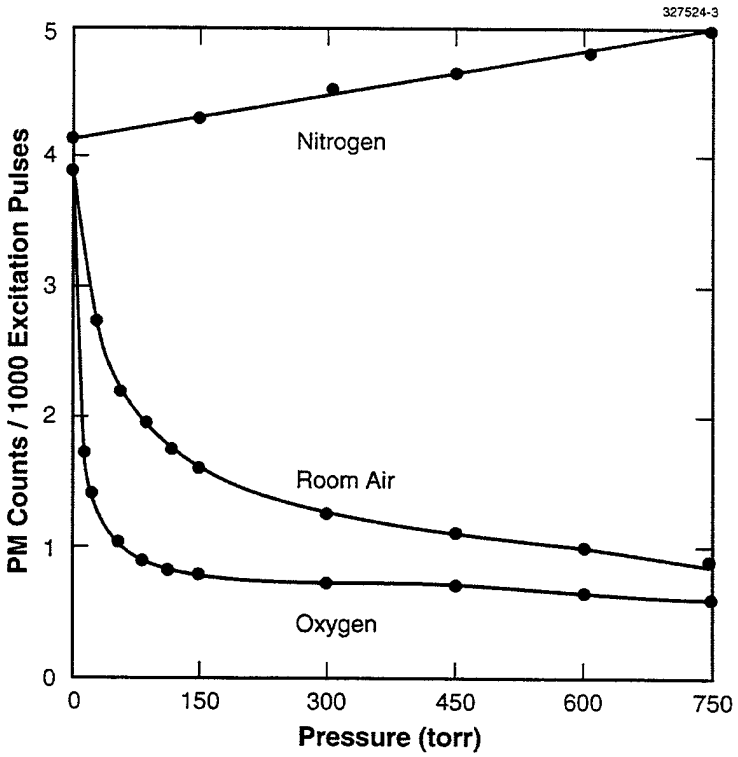

Figure 3. Fluorescence signal (in terms of photomultiplier tube counts/1000 excitation pulses) plotted against pressure of nitrogen, room air, and oxygen.

To confirm that the observed fluorescence was originating from a region of the gas in the direct path of the 266-nm excitation beam, we measured Rayleigh scattering and fluorescence signals as a function of the displacement of the focusing lens in a direction perpendicular to the plane of Figure 1, as shown in Figure 4. The displacement of the focusing lens results in a displacement of the image of the excitation beam across the narrow dimension of the slit placed in front of the photomultiplier tube. Figure 5 shows the results for Rayleigh scattering due to nitrogen at 750 torr, and fluorescence under nominal vacuum and nitrogen at 750 torr. The observed decrease of the signals from their value with the lens in the optimum position confirms that the fluorescence signal arises from the material excited by the direct excitation beam and not from the walls of the gas cell due to scattered radiation incident upon the walls.

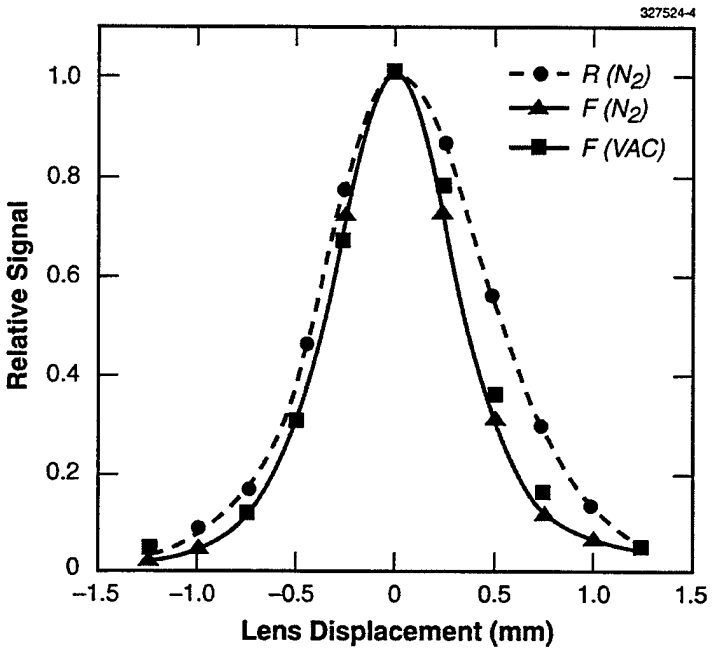

Figure 4. Normalized Rayleigh scattering and fluorescence signals vs displacement of the focusing lens in a direction perpendicular to the plane of Figure 1.

To obtain further evidence for oxygen quenching, we have measured the temporal decay of the fluorescence signal observed with gas cell under nominal vacuum and filled with oxygen at a pressure of 750 torr. Fluorescence signal decay data shown in Figure 5 was obtained using gate widths of 5 ns and gate delay increments of 5 ns. Under nominal vacuum, the plot of the fluorescence signal on a logarithmic scale vs delay time on a linear scale is fit to two straight lines whose slopes yield fluorescence lifetimes of 15 and 32 ns as shown in Figure 5. Similarly, the the fluorescence decay data obtained with oxygen at 750 torr yields fluorescence lifetimes of 5 and 31 ns. This implies that the shorter fluorescence lifetime of 15 ns under nominal vacuum is reduced to 5 ns due to the presence of oxygen in the gas cell. On the other hand, the longer fluorescence lifetime of 32 ns remains unchanged by the presence of oxygen in the gas cell.

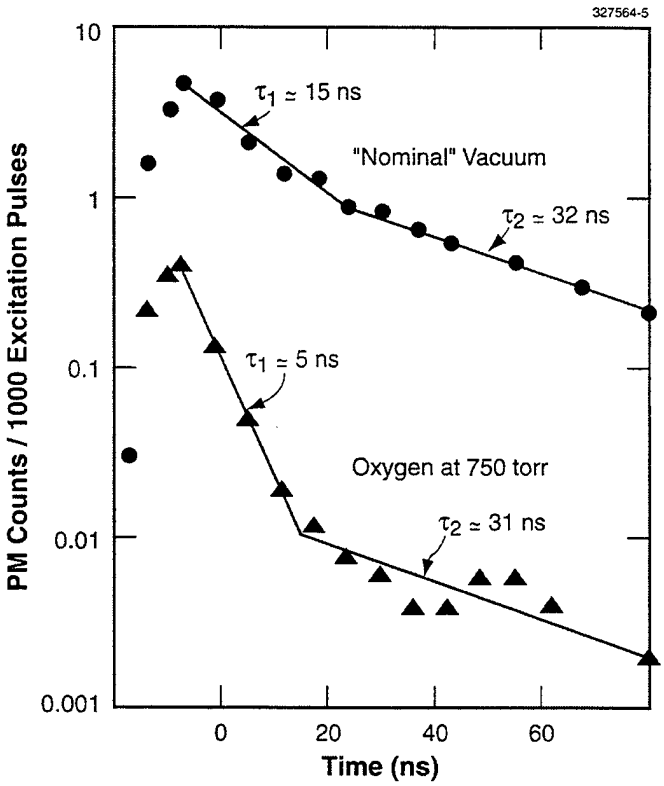

Figure 5. Fluorescence signal (in terms of photomultiplier tube counts/1000 excitation pulses) measured with a gated photon counter and plotted on a logarithmic scale as a function of time on a linear scale under nominal vacuum and oxygen at 750 torr.

Oxygen is known to be a strong quencher of fluorescence due to hydrocarbons. According to an expert [7] in this field, only one collision between a hydrocabon molecule and an oxygen molecule is required to quench the fluorescence in most cases. Therefore, the fluorescence observed in our experiment may be largely due to residual hydrocarbons in the gas cell; vacuum pump oil is a likely source of these residual hydrocarbons. The collision cross section σ_Q for oxygen quenching may be deduced as follows: The ratio of quenched fluorescence to unquenched fluorescence is given by

$$F_Q / F_o = 1/(1+\tau_o Q) \ , \tag{2}$$

where τ_o is the unquenched fluorescence lifetime, and Q is the oxygen quenching rate given by

$$Q = \sigma_Q \langle v \rangle n \ . \tag{3}$$

Here $\langle v \rangle = (8kT/\pi M)^{1/2}$ is the average velocity of oxygen molecules, k is the Boltzmann constant, T is the temperature of the gas in the cell, M is the molecular weight of oxygen, n = p/kT is the concentration of the oxygen molecules, and p is the pressure of oxygen. Equation (3) may be rewritten as

$$Q = \sigma_Q(8/\pi MkT)^{1/2}p \ . \tag{4}$$

Thus σ_Q is given by

$$\sigma_Q = (1/\tau_o p_{1/2})(\pi MkT/8)^{1/2} \ , \tag{5}$$

where $p_{1/2}$ is the pressure at which $F_Q = F_o/2$. Using the values $\tau_o = 15$ ns, $p_{1/2} = 20$ torr $= 2.7 \times 10^3$ Pa, $M = 5.3 \times 10^{-26}$ kg, $k = 1.38 \times 10^{-23}$ J/K, and $T = 295$ K, we deduce a value for $\sigma_Q = 1.5 \times 10^{-15}$ cm^2 which corresponds to an effective hardball collision diameter of 4.4×10^{-8} cm.

Unquenched fluorescence cross section is given by

$$\sigma_F = (F_o/R_s)(n_R/n_F)\sigma_R \ , \tag{6}$$

where R_s is the Rayleigh scattering signal, n_R is the molecular concentration of the gas for Rayleigh scattering, n_F is the molecular concentration for fluorescence, and σ_R is the cross section for Rayleigh scattering. Using $F_o/R_s(N_2) = 1 \times 10^{-4}$, $n_R/n_F = p(N_2)/p(F) \sim 1 \times 10^8$, $\sigma_R(N_2) = 1 \times 10^{-25}$ cm^2, we obtain $\sigma_F \sim 1 \times 10^{-21}$ cm^2 which is several orders of magnitude larger than the Rayleigh scattering cross section for nitrogen.

The ratio of quenched to unquenched fluorescence signals should vary linearly with the partial pressure of the quenching gas, as can be easily seen from Eqs. (2) and (4). However, a plot of F_0/F_Q vs p for oxygen and room air, as shown in Figure 6, exhibits significant deviation from the linear behavior for $p > 30$ torr in the case of oxygen, and for $p > 90$ torr in the case of room air. The dashed lines represent the linear fit to the data at low pressures whereas the solid lines simply represent smooth curves through the data points. Deviation from the linear behavior at higher pressures may imply that a part of the fluorescence has a considerably weak quenching rate. This is consistent with the observation that the longer fluorescence lifetime (32 ns) remains unchanged by oxygen, as shown in Figure 5. The ratio of the slopes of the dashed lines for room air and oxygen is equal to 0.17, compared with the expected value of 0.19 based on the partial pressure of oxygen in room air and the observed increase of the fluorescence signal with pressure as shown in Figure 3.

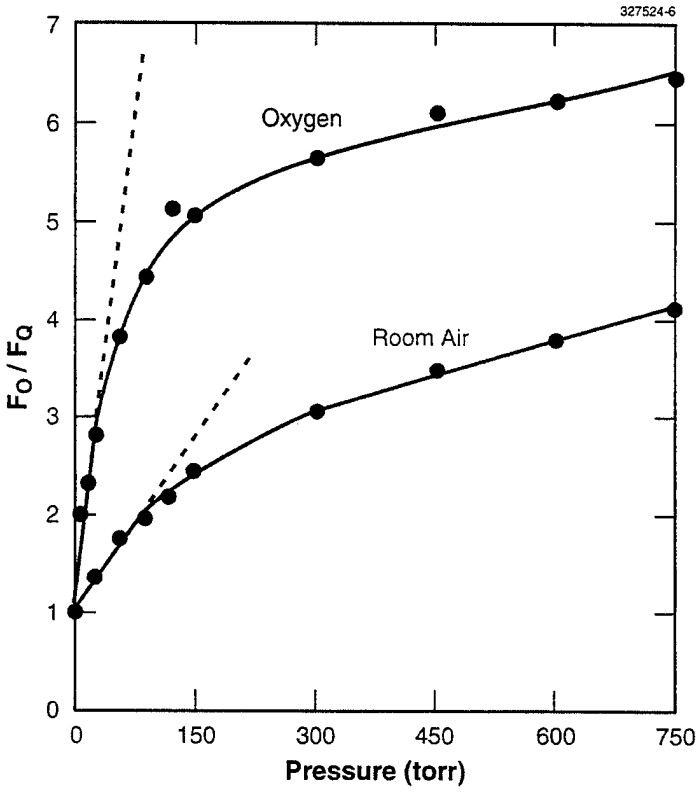

Figure 6. Ratio of unquenched to quenched fluorescence signals F_O/F_Q plotted as a function of pressure for oxygen and room air. The dashed lines represent the linear fit to the data at low pressures whereas the solid lines simply represent smooth curves through the data points.

5. CONCLUSIONS

Background fluorescence in our biodetector may be due to the presence of residual hydrocarbons in the atmospheric air. Multicity mean annual concentration of some hydrocarbons in air monitored by the United States Environmental Protection Agency (EPA) is given in Table 2, based on the data of 13 October, 1998 provided by Rhonda Thompson [8] for the 26 cities listed in Table 3. Using the results in Table 2, the total mean concentration of hydrocarbons in urban air is approximately 3×10^{11}, corresponding to 10 ppb by number of air molecules. In order to estimate the background fluorescence signal in our biodetector due to hydrocarbons in the ambient air, we need values of the fluorescence cross sections integrated over the spectral range of our biodetector from 300 to 650 nm with 266-nm excitation wavelength. This information is not readily available. It may be possible to deduce some of this information with considerable effort by using published data from several sources. A back-of-the envelope order-of-magnitude estimate for the integrated fluorescence cross section from 300 to 650 nm is 1×10^{-21} cm^2, using values of 0.5×10^{-18} cm^2 for the absorption cross section [9], 0.01 for the fluorescence quantum yield in the 300–650-nm wavelength range, and 0.2 for the fluorescence quenching factor due to air at atmospheric pressure. Using this value of 1×10^{-21} cm^2 for the fluorescence cross section, we estimate a value of 4 photons/excitation pulse for the background fluorescence signal in our biodetector, consistent with the observed value of 4 photons/excitation pulse.

The contribution of Rayleigh scattering of air to the elastic scattering channel in our single-pass biodetector with f# of ~1 and 266-nm pulse energy of ~200 nJ is estimated to be 4×10^4 photons/excitation pulse, compared with the observed background value of 5×10^4 photons per excitation pulse in the elastic channel. This shows that Rayleigh scattering of air is the dominant source of background elastic scattering in our biodetector.

TABLE 2

Multiyear, Multisite, Multicity Annual Mean Concentrations of Some Hydrocarbons in Air Monitored by EPA (13 October 1998 Data)

EPA No.	CAS No.	Hydrocarbon Air Pollutant	Formula	Mean Concentration n (cm^{-3})
43205	115-07-1	1-Propene	C_3H_6	5×10^{10}
43206	74-86-2	Acetylene	C_2H_2	2×10^{10}
43218	106-99-0	1, 3-Butadiene	C_4H_6	4×10^{9}
43231	110-54-3	Hexane	C_6H_{14}	8×10^{9}
43233	111-65-9	Octane	C_8H_{18}	4×10^{9}
43502	50-00-0	Formaldehyde	CH_2O	2×10^{10}
43504	123-38-6	Propionaldehyde	C_3H_6O	2×10^{9}
43551	67-64-1	Acetone	C_3H_6O	5×10^{10}
43505	107-02-8	2-Propenal	C_3H_4O	1×10^{9}
43801	74-87-3	Chloromethane	CH_3Cl	4×10^{9}
43802	75-09-2	Dichloromethene	CH_2Cl_2	6×10^{9}
43803	67-66-3	Chloroform	$CHCl_3$	1×10^{9}
43812	75-00-3	Ethyl Chloride	C_2H_5Cl	2×10^{9}
43814	71-55-6	1,1, 1-Trichloroethane	$C_2H_3Cl_3$	6×10^{9}
43815	107-06-2	1, 2-Dichloroethane	$C_2H_4Cl_2$	2×10^{9}
43819	74-83-9	Methyl bromide	CH_3Br	1×10^{9}
43820	79-00-5	1,1, 2-Trichloroethane	$C_2H_3Cl_3$	1×10^{9}
43824	79-01-6	Trichloroethylene	C_2HCl_3	2×10^{9}
43826	75-35-4	1, 1-Dichloroethylene	$C_2H_2Cl_2$	1×10^{9}
43828	156-60-5	(t) 1, 2-Dichloroethylene	$C_2H_2Cl_2$	1×10^{9}
43830	10061-02-6	(t) 1, 3-Dichloropropylene	$C_2H_4Cl_2$	1×10^{9}
43831	10061-01-5	(cis) 1, 3-Dichloropropylene	$C_3H_4Cl_2$	7×10^{9}
43835	126-99-8	2-Chloro-1, 3-butadiene	C_4H_5Cl	1×10^{9}
43860	75-01-4	Vinyl chloride	C_2H_3Cl	3×10^{9}
45201	71-43-2	Benzene	C_6H_6	1×10^{10}
45202	108-88-3	Toluene	C_7H_8	3×10^{10}
45203	100-41-4	Ethylbenzene	C_8H_{10}	5×10^{9}
45204	95-47-6	o-Xylene	C_8H_{10}	5×10^{9}
45205	108-38-3	m-Xylene	C_8H_{10}	9×10^{9}
45206	106-42-3	1, 1-Dimethylbutylbenzene	$C_{12}H_{18}$	7×10^{9}
45208	95-63-6	1, 2, 4-Trimethylbenzene	C_9H_{12}	6×10^{9}
45210	98-82-8	1-Methylethylbenzene	C_9H_{12}	4×10^{9}
45220	100-42-5	Styrene	C_8H_8	4×10^{9}
45801	100-90-7	Chlorobenzene	C_6H_5Cl	1×10^{9}
45805	95-50-1	o-Dichlorobenzene	$C_6H_4Cl_2$	2×10^{9}
45806	541-73-1	m-Dichlorobenzene	$C_6H_4Cl_2$	2×10^{9}
45807	106-46-7	p-Dichlorobezene	$C_6H_4Cl_2$	4×10^{9}

TABLE 3

List of Cities Included in the Database for the Hydrocarbons, as Given in Table 2

Atlanta, GA
Baltimore, MD
Baton Rouge, LA
Beaumont, TX
Birmingham, AL
Burlington, VT
Chicago, IL
Cleveland, OH
Dallas, TX
Detroit, MI
Fort Lauderdale, FL
Gary, IN
Houston, TX
Jacksonville, FL
Los Angeles, CA
Louisville, KY
Miami, FL
Orlando, FL
Pensacola, FL
Philadelphia, PA
Portland, OR
St. Louis, MO
San Francisco, CA
Toledo, OH
Washington, DC
Wichita, KS

REFERENCES

1. Lord Rayleigh, "Scattering of Light by Small Particles," *Phil. Mag.* **41**, 447 (1871).
2. A. T. Young, "Rayleigh Scattering," *Appl. Optics* **20**, 533 (1981).
3. A. T. Young, "Rayleigh Scattering," *Physics Today*, January 1982, p. 42.
4. R. R. Rudderland and D. R. Bach, "Rayleigh Scattering of Ruby-Laser Light by Natural Gases," *J. Opt. Soc. Am.* **58**, 1260 (1968).
5. Shardanand and A. D. P. Rao, "Absolute Rayleigh Scattering Cross Sections of Gases and Freons of Stratospheric Interest in the Visible and ultraviolet Regions," NASA Tech. Note D-8442, March 1977.
6. D. R. Bates, "Rayleigh Scattering from Air," *Planet. Space Sci.* **32**, 785 (1984).
7. L. A. Melton, Department of Chemistry, University of Texas, Richardson, TX, private communication, 1998.
8. R. Thompson, EPA Office of Air Quality, Planning, and Standards, Research Triangle Park, NC, private communication, 1999.
9. M. Suto, X. Wang, J. Shan, and L. C. Lee, "Quantitative Photoabsorption and Fluorescence Spectroscopy of Benzene, Napthalene, and some Derivatives at 106-295 nm," *J. Quant. Spectrosc. Radiat. Transfer* **48**, 79 (1992).

REPORT DOCUMENTATION PAGE

Form Approved
OMB No. 0704-0188

1. AGENCY USE ONLY (*Leave blank*)	2. REPORT DATE	3. REPORT TYPE AND DATES COVERED
	17 May 1999	Technical Report

4. TITLE AND SUBTITLE

Background Fluorescence in an Aerosol Biodetector Based on 266-nm Excitation

5. FUNDING NUMBERS

C — F19628-95-C-0002

6. AUTHOR(S)

Roshan L. Aggarwal

7. PERFORMING ORGANIZATION NAME(S) AND ADDRESS(ES)

Lincoln Laboratory, MIT
244 Wood Street
Lexington, MA 02420-9108

8. PERFORMING ORGANIZATION REPORT NUMBER

TR-1052

9. SPONSORING/MONITORING AGENCY NAME(S) AND ADDRESS(ES)

U.S. Army/ERDEC
CBDCOM-ERDEC
Attn: SCBRD-RTE
Aberdeen Proving Grounds, MD 21010-5423

10. SPONSORING/MONITORING AGENCY REPORT NUMBER

ESC-TR-98-045

11. SUPPLEMENTARY NOTES

None

12a. DISTRIBUTION/AVAILABILITY STATEMENT

Approved for public release; distribution is unlimited.

12b. DISTRIBUTION CODE

13. ABSTRACT (*Maximum 200 words*)

Background fluorescence in an aerosol biodetector based on 266-nm excitation has been investigated, using a gas cell which could be evacuated and then filled with a gas (of interest) at a known pressure. A frequency-quadrupled, Q-switched Nd:YAG microchip laser with a pulse width of less than 1 ns and a pulse repetition rate of ~10^4 pps was used to measure both fluorescence and Rayleigh scattering in a direction at 90° to the 266-nm excitation beam, as a function of the gas pressure for nitrogen, oxygen, and room air. Rayleigh scattering was also measured for helium and xenon gases. The relative Rayleigh scattering cross sections measured in this work are consistent with their previously reported values, ensuring that the observed fluorescence was originating from a region of the gas in the direct path of the 266-nm excitation beam. Fluorescence signal observed in the spectral range of interest 300–650 nm under nominal vacuum conditions (~1×10^{-5} torr) exhibited strong quenching upon filling the gas cell with oxygen, but not with nitrogen. Strong oxygen-induced quenching leads us to believe that the background fluorescence is due, at least in part, to the presence of residual hydrocarbons in the atmospheric air. An order-of-magnitude calculation, based on an estimated value of fluorescence cross section of 1×10^{-21} cm^2, oxygen quenching factor of 0.2 for atmospheric air, and concentration of 10 ppb for hydrocarbons in urban air, is consistent with the observed value of ~4 photons per excitation pulse for the background fluorescence signal in our single-pass biodetector with f# of ~1 and 266-nm pulse energy of ~200 nJ.

14. SUBJECT TERMS			15. NUMBER OF PAGES
biodetector	hydrocarbons in urban air	Rayleigh scattering of gases	27
fluorescence biodetector	UV excitation	fluorescence cross section	
aerosol biodetector	fluorescence	fluorescence of hydrocarbons	16. PRICE CODE
266-nm excitation	background fluorescence	fluorescence quenching	
	fluorescence lifetime	oxygen quenching of fluorescence	

17. SECURITY CLASSIFICATION OF REPORT	18. SECURITY CLASSIFICATION OF THIS PAGE	19. SECURITY CLASSIFICATION OF ABSTRACT	20. LIMITATION OF ABSTRACT
Unclassified	Unclassified	Unclassified	Same as Report